Inorganica Chimica Acta 387 (2012) 86–92

Contents lists available at SciVerse ScienceDirect

Inorganica Chimica Acta

journal homepage: www.elsevier.com/locate/ica

Synthesis, reactivity, thermal, electrochemical and magnetic studies on iron(III) complexes of tetradentate Schiff base ligands

Chira R. Bhattacharjee [a,*], Pankaj Goswami [b], Paritosh Mondal [a]

[a] Department of Chemistry, Assam University, Silchar 788011, Assam, India
[b] Department of Chemistry, Silchar Polytechnic, Silchar 788015, Assam, India

ARTICLE INFO

Article history:
Received 24 September 2011
Received in revised form 22 December 2011
Accepted 29 December 2011
Available online 9 January 2012

Keywords:
Schiff base
2-Hydroxy-1-naphthaldehyde
Ethylenediamine
o-Phenylenediamine
Iron(III) complexes
DFT

ABSTRACT

Cationic iron(III) complexes of the type $[FeL^n(H_2O)_2]NO_3$ (n = 1 or 2) were accessed from the interaction of $Fe(NO_3)_3{\cdot}9H_2O$ with $[N_2O_2]$ donor Schiff base (L) in 1:1 molar ratio. The Schiff base ligands were prepared from condensation of 2-hydroxy-1-naphthaldehyde with *o*-phenylenediamine or ethylenediamine in 2:1 molar ratio. Reaction of the aquated complexes with neutral N-donor molecules (X) viz. imidazole, benzimidazole and pyridine led to substitution of weakly held axial aquo groups affording new mixed ligand complexes, $[FeL^nX_2]NO_3$. The compounds were characterized by elemental analyses, FT-IR, UV–Vis, solution electrical conductivity, FAB mass, ^1H and ^{13}C NMR (ligands only) spectroscopy. The thermal study provided unambiguous evidence for the occurrence of coordinated water in the complexes. Room temperature magnetic susceptibility measurements are consistent with high spin octahedral iron(III) complexes. Cyclic voltammetry revealed a quasi-reversible one electron redox response ($\Delta E_p > 100$ mV) assignable to Fe(III)/Fe(II) couple with negative half wave potential. The ground state geometries of the aquo complex, $[FeL^2(H_2O)_2]NO_3$ and pyridine complex, $[FeL^2(Py)_2]NO_3$ were ascertained by density functional theory using DMOL3 program with BLYP functional.

1. Introduction

Metal–Schiff base complexes have continued to enjoy extensive interest owing to their structural diversity and potential applications in pharmacology and catalysis. The design, synthesis, and characterization of iron complexes with Schiff-base ligands play a vital role in the coordination chemistry of iron due to their importance as biomimetic models for iron-containing enzymes [1,2], oxidation catalysts [3–5], and molecular materials based on temperature, pressure, or light-induced spin crossover behavior [6–9]. Attention has been devoted in recent years to the mixed-ligand complexes of transition metals containing nitrogen donors [10–12] with potential applications as separation materials, catalysts, precursors, models for understanding enzyme catalysis [13–16] and interesting structures [17–19]. Mixed-ligand complexes containing N, O, and/or S donors are important owing to their antifungal, antibacterial, and anticancer activities [20]. Use of iron–Schiff-base complexes in different catalytic reactions have been documented [21–24]. Although a large number of metal–$[N_2O_2]$ compounds exist [25–28], reports on corresponding Fe(III) complexes are scarce. Mostly divalent metal ions have been used for the complexation with diprotic Schiff base ligands having $[N_2O_2]$ core [29–31]. Iron(III) tridentate Schiff-base complexes have been employed as efficient catalysts for the oxidation of sulfides to sulfoxides by urea hydrogen peroxide [32].

Recently, we have reported aquated iron(III) complex of a quadridentate $[N_2O_2]$ donor Schiff base and its ligand (aquo) exchange reactions with different inorganic donor anions yielding new mixed-ligand complexes [33] and some mixed-ligand mono- and dinuclear iron(III) and oxovanadium(IV) complexes with tridentate [ONO] donor Schiff base ligand [34]. Substitution of weakly bound ethanol at the axial site of iron(III) Schiff base complexes by neutral N-donor ligands producing new mixed ligand complexes have been reported by us very recently [35].

Accordingly we intend to report here the synthesis, thermal, electrochemical and magnetic studies of iron(III) complexes with the $[N_2O_2]$ donor Schiff bases derived from the condensation of 2-hydroxy-1-naphthaldehyde with *o*-phenylenediamine or ethylenediamine. Reactivity studies of the complexes with neutral N-donor molecules viz. imidazole, benzimidazole and pyridine as an access to new mixed ligand Schiff base complexes have also been incorporated.

2. Experimental

2.1. Physical measurements

Microanalytical (CHN) data were obtained with a Perkin Elmer model 240C elemental analyzer. Solid state infrared spectra were

* Corresponding author. Tel.: +91 9435175671; fax: +91 3842270803.
E-mail address: crbhattacharjee@rediffmail.com (C.R. Bhattacharjee).

0020-1693/$ - see front matter © 2012 Elsevier B.V. All rights reserved.
doi:10.1016/j.ica.2011.12.056

recorded with a Perkin Elmer/spectrum BX series FT-IR spectrophotometer using KBr pellets in the range 4000–400 cm^{-1}. Electronic spectra were recorded in dichloromethane solution on a Shimadzu 1600 PC UV–Vis spectrophotometer in 200–800 nm range. NMR spectra were acquired from Bruker Advance 300 MHz FT NMR spectrophotometer using $CDCl_3$ as solvent and TMS as internal standard. FAB mass spectra were recorded on JEOL SX-102 Mass spectrometer. TGA/DTA was carried out on a PYRIS DIAMOND thermal analyzer under a dynamic flow of nitrogen (100 ml/min) and heating rate of 10 °C/min from ambient temperature to 1000 °C. Molar conductances of the Schiff base complexes were measured on Systronics direct reading conductivity meter type CM-82. Magnetic susceptibilities of the complexes were measured at room temperature on a Lakeshore 7407 Vibrating Sample Magnetometer in the range −20000 to +20000 gauss and diamagnetic corrections were made using Pascal's constants. Electrochemical behavior of the complexes were examined by cyclic voltammetry at room temperature in acetonitrile solution (*ca.* 10^{-3}) M using TBAP as supporting electrolyte under dry N_2 atmosphere on a PC controlled CHI model 660C electrochemical workstation. A Pt disk, a Pt-wire auxiliary electrode and an aqueous SCE were used in a three electrode configuration.

2.2. Materials

Solvents used were purified by standard methods described in the literature [36,37]. Commercially available pure samples of 2-hydroxy-1-naphthaldehyde, *o*-phenylenediamine and ethylenediamine were obtained from Fluka A.G., Switzerland and used as received. Metal salts were procured from Fisher Scientific Chemicals, India and used as received.

2.3. Synthesis of Schiff base ligands (H_2L^1 and H_2L^2)

The Schiff base ligands were synthesized by refluxing methanolic solution of *o*-phenylenediamine (10 mmol, 1.08 g) or ethylenediamine (10 mmol, 0.60 g) with 2-hydroxy-1-naphthaldehyde (20 mmol, 3.44 g) in 30 mL methanol in presence of few drops of acetic acid. On cooling, the orange (H_2L^1) or yellow (H_2L^2) crystals formed were filtered and washed with ether. Recrystallization from ethanol afforded pure Schiff bases (Scheme 1).

Ligand ***H_2L^1***: Yield: 78%. *Anal.* Calc. for $C_{28}H_{20}N_2O_2$: C, 80.76; H, 4.81; N, 6.73. Found: C, 80.24; H, 4.78; N, 6.38%. FT-IR (KBr, cm^{-1}): $\nu_{(C-O)}$ = 1319, $\nu_{(C=N)}$ = 1629, $\nu_{(O-H)}$ = 3428. UV–Vis, λ_{max} (nm) [ε_{max} (M^{-1} cm^{-1})] (CH_2Cl_2): 454 (11320), 376 (18700), 322 (17820), 244 (43580). ^1H NMR ($CDCl_3$, TMS, δ ppm): 15.05 (s, 1H, –OH); 9.46 (s, 1H, –HC=N); 6.83–8.44 (m, 16H, phenyl proton); ^{13}C NMR ($CDCl_3$, TMS, δ ppm): 39.21, 39.49, 39.77, 40.04, 40.35, 118.79, 121.51, 123.30, 127.14, 127.79, 128.98, 136.25, 155.96, 168.48. MS (FAB, *m*/*z*): 416$[M]^+$.

Ligand ***H_2L^2***: Yield: 73%. *Anal.* Calc. for $C_{24}H_{20}N_2O_2$: C, 78.26; H, 5.43; N, 7.61. Found: C, 78.46; H, 5.62; N, 7.61%. FT-IR (KBr, cm^{-1}): $\nu_{(C-O)}$ = 1327, $\nu_{(C=N)}$ = 1617, $\nu_{(O-H)}$ = 3428. UV–Vis, λ_{max} (nm) [ε_{max} (M^{-1} cm^{-1})] (CH_2Cl_2): 404 (11100), 350 (12800), 313 (17000), 241 (49700). MS (FAB, *m*/*z*): 368$[M]^+$.

2.4. Synthesis of iron(III) complexes, $[FeL^n(H_2O)_2]NO_3$, n = 1, 2 (***1*** and ***2***)

$Fe(NO_3)_3{\cdot}9H_2O$ (2 mmol, 0.808 g) solution in methanol (20 mL) was added to a solution of the corresponding Schiff base H_2L^1 (2 mmol, 0.832 g) or H_2L^2 (2 mmol, 0.736 g) in 20 mL methanol and the reaction mixture was stirred for 4 h. On cooling, dark brown microcrystalline solid formed was filtered, washed with cold ethanol, recrystallized from ethanol and dried in vacuum over anhydrous $CaCl_2$ (Scheme 2).

Complex ***1***: Yield: 67%. *Anal.* Calc. for $FeC_{28}H_{22}N_3O_7$: C, 59.15; H, 3.87; N, 7.39. Found: C, 58.95; H, 3.78; N, 7.68%. FT-IR (KBr, cm^{-1}): $\nu_{(Fe-O)}$ = 499, $\nu_{(Fe-N)}$ = 553, ρ_{wagg} (H_2O) = 617, ρ_{rock} (H_2O) = 853, $\nu_{(C-O)}$ = 1338, $\nu_{(N-O)}$ (free NO_3^-) = 1385, $\nu_{(C=N)}$ = 1597, $\nu_{(O-H)}$ (H_2O) = 3418. UV–Vis, λ_{max} (nm) [ε_{max} (M^{-1} cm^{-1})] (CH_2Cl_2): 513 (1500), 342 (8200), 248 (11800). MS (FAB, *m*/*z*): 568$[M]^+$, 532 $[M-2H_2O]^+$, 470. Λ_m(DMSO, Ω^{-1} cm^2 mol^{-1}): 53.4. μ_{eff} (B.M.): 5.94.

Complex ***2***: Yield: 62%. *Anal.* Calc. for $FeC_{24}H_{22}N_3O_7$: C, 55.38; H, 4.23; N, 8.07. Found: C, 55.24; H, 4.38; N, 8.18%. FT-IR (KBr, cm^{-1}): $\nu_{(Fe-O)}$ = 515, $\nu_{(Fe-N)}$ = 565, ρ_{wagg} (H_2O) = 604, ρ_{rock} (H_2O) = 869, $\nu_{(C-O)}$ = 1339, $\nu_{(N-O)}$ (free NO_3^-) = 1384, $\nu_{(C=N)}$ = 1605, $\nu_{(O-H)}$ (H_2O) = 3434. UV–Vis, λ_{max} (nm) [ε_{max} (M^{-1} cm^{-1})] (CH_2Cl_2): 517 (400), 473 (420), 359 (8130), 319 (12060), 244 (21110). MS (FAB, *m*/*z*): 520$[M]^+$, 484 $[M-2H_2O]^+$, 422. Λ_m (DMSO, Ω^{-1} cm^2 mol^{-1}): 51.8. μ_{eff} (B.M.): 5.91.

2.5. Reactivity studies

The complex, $[FeL^n(H_2O)_2]NO_3$ (1 mmol) was dissolved in ethanol (20 mL) and was added to an ethanolic solution (20 mL) of imidazole, benzimidazole or pyridine (2 mmol) separately. The reaction mixture was stirred on a water bath for 45 min. The resulting brown micro crystalline solid was filtered, washed with cold ethanol, recrystallized from methanol-dichloromethane and dried in vacuum over anhydrous $CaCl_2$ (Scheme 3).

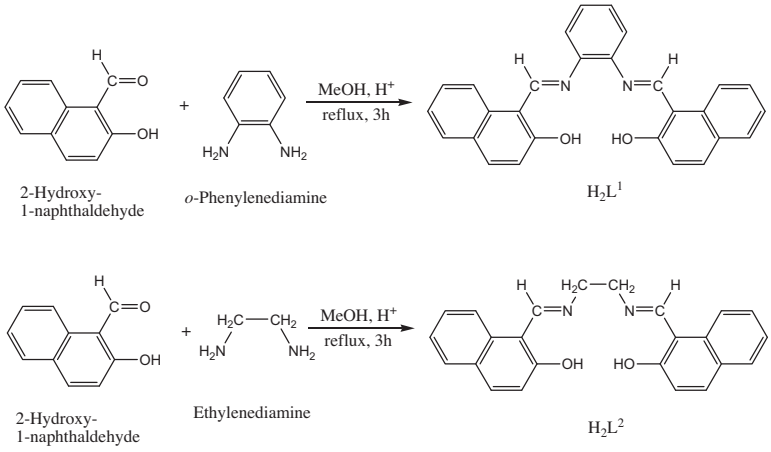

Scheme 1. Synthesis of Schiff base ligands.

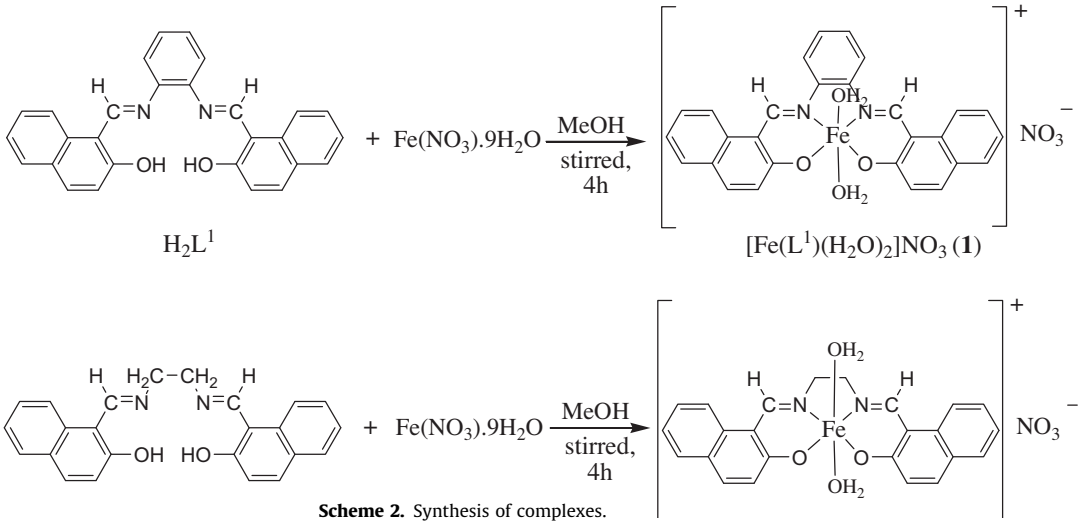

Scheme 2. Synthesis of complexes.

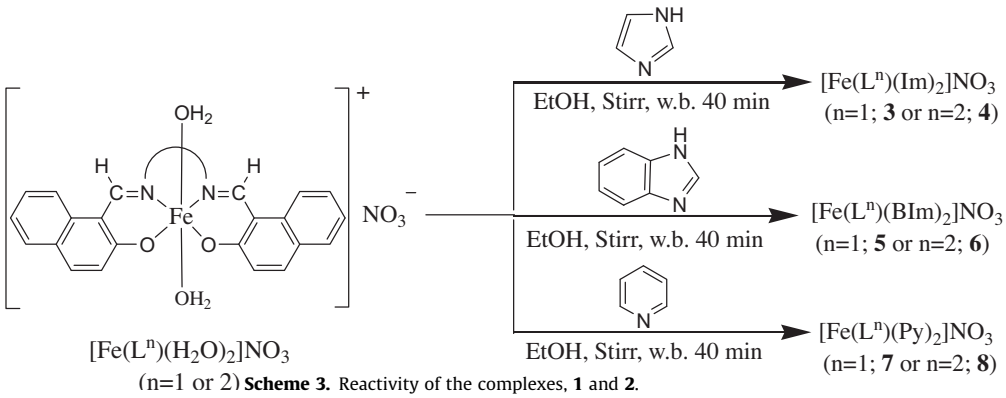

Scheme 3. Reactivity of the complexes, **1** and **2**.

3. Results and discussion

The ligands and complexes including those accessed through reactivity studies, are stable to air and moisture. Though ionic in character, the compounds are soluble in dichloromethane, chloroform as well as in acetonitrile, DMF, DMSO and ethanol. We presume that such solubility behavior arises due to higher hydrocarbon content (>75%) of the compounds. The Schiff base ligand H_2L^2, however, was very poorly soluble in these solvents. The analytical data are in good agreement with the proposed formulae of the Schiff base ligands and their complexes. Two molecules of water were found to coordinate to the metal center in the complexes. Efforts to obtain diffraction quality single crystal by using slow evaporation in different solvents, solvent diffusion method or replacing the counter anion by BF_4^- or ClO_4^- did not prove successful.

3.1. Infrared spectra

The free ligands showed stretching modes attributed to C=N, C–O and O–H at *ca.* 1620, 1320 and 3428 cm^{-1}, respectively. On complexation, the C=N band shifts to lower wave number, indicating coordination through the azomethine nitrogen [38]. The participation of phenolic oxygen and azomethine nitrogen in the complexes is further supported by prominent IR peaks for ν(M–O) and ν(M–N) in the ranges 499–515 and 553–565 cm^{-1}, respectively [39]. Presence of coordinated water in the complexes were confirmed by a broad band at *ca.* 3425 cm^{-1} for ν(O–H) with two weak bands at *ca.* 610 and 860 cm^{-1} attributable to wagging and rocking modes of coordinated water, respectively [40]. A strong band around 1385 cm^{-1} assignable to ν_{N-O}(asy) is typical of uncoordinated nitrate [41].

3.2. UV–Vis spectra

The electronic spectra of the ligands and the complexes recorded in dichloromethane exhibited high intensity bands in the range 244–359 nm attributed to intra-ligand $\pi \rightarrow \pi^*$ and $n \rightarrow \pi^*$ transitions [42]. Very low intensity bands in the range 473–517 nm in the complexes are anticipated to arise from partly allowed d–d transition ($^6A_1 \rightarrow$ excited states) confirming the occurrence of high spin octahedral Fe(III) center [43].

3.3. NMR spectra

The NMR spectra of Schiff base ligand H_2L^1 were recorded in $CDCl_3$ at room temperature. The ^1H NMR spectral data (vide infra) of the ligand H_2L^1 showed a sharp singlet at 9.46 ppm assignable to protons of the azomethine group (–CH=N–). Multiplet in the range 6.83–8.44 ppm is due to protons of the benzene ring. A sharp singlet in the downfield region at 15.05 ppm is attributed to hydroxyl protons. The ^{13}C NMR spectra of the ligand is concordant with different types of magnetically non-equivalent carbons. The peak at 168.48 ppm is due to azomethine carbon (–CH=N–). NMR spectra of the ligand H_2L^2 could not be recorded due to very poor solubility of the compound in $CDCl_3$ as well as DMSO.

Table 1
TGA data of the complex **2**.

Complex	TG plateau (°C)	DTG (°C)	Mass loss (%)		Process
			Expl.	Calc.	
$[Fe(L^2)(H_2O)_2]NO_3$	135–164	147	6.88	6.92	loss of two molecules of coordinated water
	164–252	244	11.87	11.92	loss of NO_3
	252–664	643	28.75	–	partial decomposition of the ligand

Table 2
DTA data of the complex 2.

Complex	Temperature range (°C)	DTA peak (°C)	ΔH (J/g)	Process
$[Fe(L^2)(H_2O)_2]NO_3$	100–185	150 exo	166.28	partial decomposition
	226–287	254 exo	64.25	partial decomposition

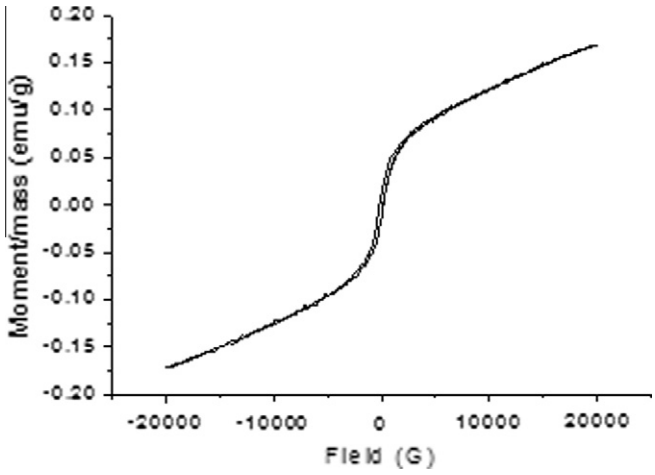

Fig. 1. Magnetization vs. magnetic field curve of the complex $[Fe(L^2)(H_2O)_2]NO_3$.

Table 3
Electrochemical data of complexes **1** and **2**.

Compounds	E_p^a (V)	E_p^c (V)	ΔE_p (V)	$E_{1/2}$ (V)
$[Fe(L^1)(H_2O)_2]NO_3$	−0.404	−0.763	0.359	−0.583
$[Fe(L^2)(H_2O)_2]NO_3$	−0.326	−0.687	0.361	−0.506

3.4. Mass spectra

The mass spectra of the compounds were recorded in FAB ionization mode. The molecular ion peak of the ligands $H_2L^1$and H_2L^2 at m/z 416 and 368, respectively, and other fragments observed were in good agreement with the proposed formula. The molecular formula $[Fe(L^1)(H_2O)_2]NO_3$ and $[Fe(L^2)(H_2O)_2]NO_3$ suggested for the complexes were confirmed by the observed molecular ion peak in the FAB mass spectra at *m/z* 568 and 520, respectively. The first fragmentation step for the complexes correspond to the loss of water molecules resulting in formation of the fragment ions $\{[Fe(L^1)]NO_3\}^+$ and $\{[Fe(L^2)]NO_3\}^+$ at *m/z* 532 and 484, respectively corroborating the occurrence of coordinated water in the complexes. Further the peak observed at *m/z* 470 and 422 for the iron (III) complexes (**1** and **2**) is attributed to the species $[Fe(L^1)]^+$ and $[Fe(L^2)]^+$, respectively, arising from the loss of NO_3^- counter ion. Thus the mass spectrometric fragmentation patterns are consistent with the proposed formulae of the aquated complexes **1** and **2**.

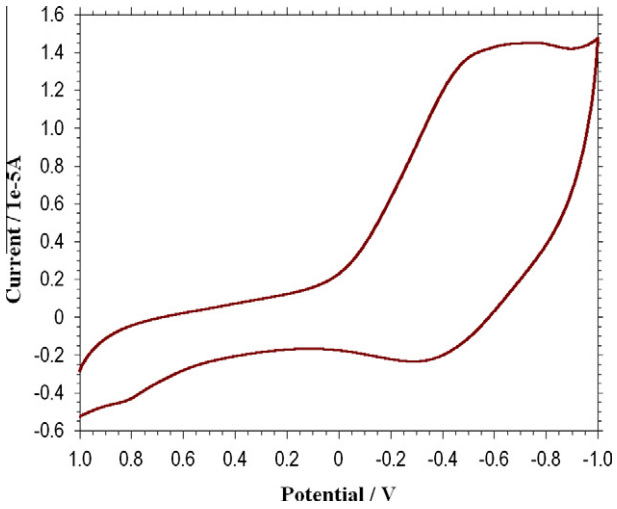

Fig. 2. Cyclic voltammogram of the complex $[Fe(L^2)(H_2O)_2]NO_3$.

3.5. Thermal study

Thermal analysis of one of the complexes, $[Fe(L^2)(H_2O)_2]NO_3$ was carried out by TG and DTA technique as a representative case. Thermal data of the complexes are presented in Tables 1 and 2. The complex underwent three-step decomposition. The first step (135–164 °C) with DTG peak at 147 °C showed a weight loss of 6.88% that corresponds to the loss of two molecules of coordinated water. The second (164–252 °C) and the third step (242–664 °C) with DTG. peak at 244 and 643 °C, respectively, corresponds to loss of nitrate ion and partial decomposition of the ligand moiety.

The exothermic changes in the temperature ranges 100–185 and 226–287 °C with DTA peak at 150 and 254 °C, respectively, is related to the decomposition of the ligand molecule.

3.6. Molar conductance

The solution electrical molar conductance of the complexes $[Fe(L^1)(H_2O)_2]NO_3$ and $[Fe(L^2)(H_2O)_2]NO_3$ in DMSO (10^{-3} M) were 53.4 and 51.8 Ω^{-1} cm^2 mol^{-1}, respectively, suggesting 1:1 electrolytic nature of the complexes [44].

3.7. Magnetic susceptibility

The magnetization versus magnetic field variation were examined in the range −20000 to +20000 Gauss and the hysteresis

Table 4
Analytical data and physical properties of complexes **3**–**8**.

Complexes	Color	Yield (%)	Elemental analysis[a] (%)			Λ (Ω^{-1} cm^2 mol^{-1})	μ_{eff} (B.M.)
			C	H	N		
$[Fe(L^1)(Im)_2]NO_3$ (**3**)	brown	62	61.35(61.08)	4.05(3.89)	14.41(14.67)	52.8	5.88
$[Fe(L^2)(Im)_2]NO_3$ (**4**)	brown	60	58.29(58.06)	4.01(4.19)	15.98(15.81)	53.1	5.83
$[Fe(L^1)(BIm)_2]NO_3$ (**5**)	brown	58	65.39(65.63)	3.81(3.91)	12.90(12.76)	55.2	5.94
$[Fe(L^2)(BIm)_2]NO_3$ (**6**)	brown	55	63.23(63.33)	4.30(4.17)	13.49(13.61)	50.9	5.92
$[Fe(L^1)(Py)_2]NO_3$ (**7**)	pale brown	63	65.85(66.09)	4.17(4.06)	9.98(10.14)	54.7	5.88
$[Fe(L^2)(Py)_2]NO_3$ (**8**)	pale brown	61	63.74(63.55)	4.53(4.36)	10.71(10.90)	57.5	5.90

[a] Calculated values are given in parenthesis.

Table 5
FT-IR (KBr, cm^{-1}), UV–Vis, λ_{max} (nm) [ε_{max} (M^{-1} cm^{-1})] and mass spectral data of complexes **3**–**8**.

Complexes	ν_{N-H} (Im/BIm)	ν_{C-H} (Py)	$\nu_{C=N}$	ν_{Fe-N}	ν_{Fe-O}	Ring modes of coordinated (Im/BIm/Py)	d–d band	CT band	Mass peak (*m*/*z*)
$[Fe(L^1)(Im)_2]NO_3$ (**3**)	3410	–	1610	553	506	1540, 1508, 1460, 1342	503 (890)	346 (5660), 317 (5500), 244 (12620)	668
$[Fe(L^2)(Im)_2]NO_3$ (**4**)	3417	–	1612	560	510	1541, 1505, 1435, 1337	519 (860)	310 (23100), 257 (27000), 237 (26800)	620
$[Fe(L^1)(BIm)_2]NO_3$ (**5**)	3414	–	1612	555	493	1510, 1480, 1455, 1441, 1427	495 (700)	361 (9100), 337 (11600), 309 (12400), 257 (24200)	768
$[Fe(L^2)(BIm)_2]NO_3$(**6**)	3403	–	1615	556	502	1522, 1482, 1464,1440, 1422	508 (770)	340 (13510), 306 (12200), 318 (11900), 295 (10080)	720
$[Fe(L^1)(Py)_2]NO_3$ (**7**)	–	3040	1610	565	503	1570, 1436, 637, 473	498 (980)	380 (5560), 340 (8700), 320 (6900), 250 (17800), 235 (20200)	690
$[Fe(L^2)(Py)_2]NO_3$ (**8**)	–	3050	1615	564	512	1576, 1410, 643, 478	496 (840)	340 (6100), 320 (5700), 290 (5530), 257 (20700), 234 (19840)	642

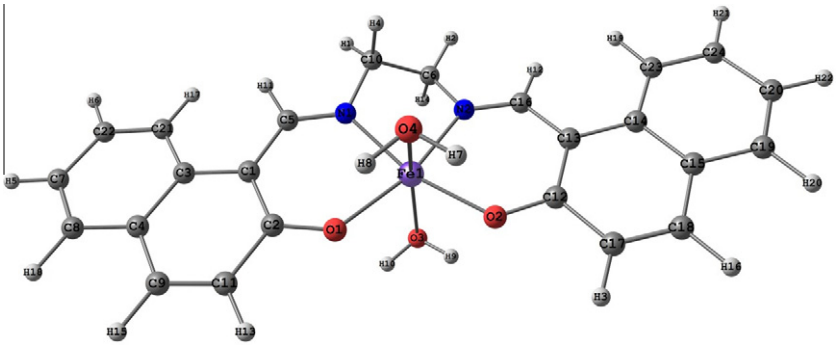

Fig. 3. DFT (BLYP/DNP) optimized geometry of the complex $[Fe(L^2)(H_2O)_2]^+$.

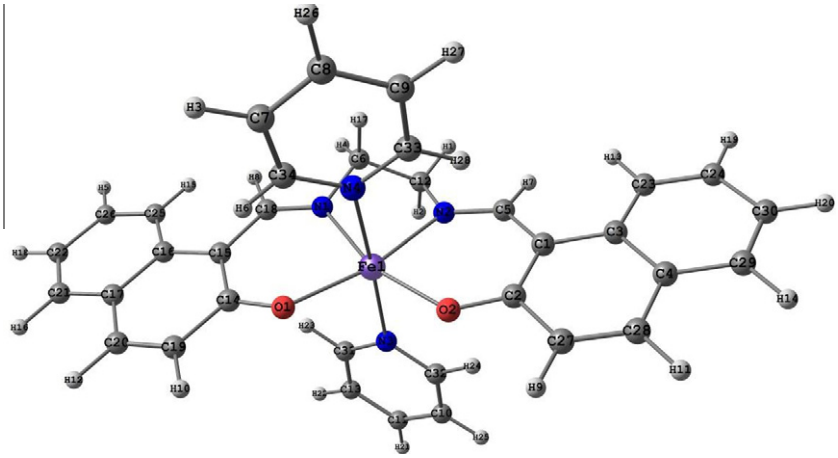

Fig. 4. DFT (BLYP/DNP) optimized geometry of the complex $[Fe(L^2)(Py)_2]^+$.

Table 6
Structurally significant geometrical parameters of complexes **1** and **8** as computed from DFT.

Bond distances (Å)			Bond angles (°)		
Bond type	$[Fe(L^2)(H_2O)_2]^+$	$[Fe(L^2)(Py)_2]^+$	Bond type	$[Fe(L^2)(H_2O)_2]^+$	$[Fe(L^2)(Py)_2]^+$
Fe(1)–N(1)	2.104	2.148	N(1)–Fe(1)–N(2)	80.20	78.79
Fe(1)–N(2)	2.104	2.145	N(1)–Fe(1)–O(1)	85.21	83.69
Fe(1)–O(1)	2.004	2.009	O(1)–Fe(1)–O(2)	109.57	113.86
Fe(1)–O(2)	2.005	2.013	O(2)–Fe(1)–N(2)	85.07	83.79
Fe(1)–O(3)	2.456	–	O(3)–Fe(1)–O(4)	158.20	–
Fe(1)–O(4)	2.465	–	N(3)–Fe(1)–N(4)	–	173.15
Fe(1)–N(3)	–	2.407	–	–	–
Fe(1)–N(4)	–	2.397	–	–	–

curve of the complex $[Fe(L^2)(H_2O)_2]NO_3$ is presented in Fig. 1 as a representative case. The effective magnetic moment of the complexes are then calculated from the initial slope of the hysteresis using the relation

$$\mu_{eff} = 2.827 \times \sqrt{(\chi'_m \times T)}, \chi'_m = \chi_m = \chi_{dia},$$

where χ_{dia} is diamagnetic correction.

The diamagnetic corrections are calculated by summing the contributions from the atoms, ions and bonds of the molecule using Pascal's constants.

The magnetic moment values of the complexes $[Fe(L^1)(H_2O)_2]NO_3$ and $[Fe(L^2)(H_2O)_2]NO_3$ at room temperature were found to be 5.94 and 5.91 B.M., respectively, in conformity with octahedral high spin (s = 5/2, d^5) configuration for the complexes.

3.8. Cyclic voltammetry

Electrochemical behavior of the complexes (**1** and **2**) were examined by cyclic voltammetry in anhydrous acetonitrile solution (10^{-3} M) containing 0.1 M tetrabutyl ammonium perchlorate (TBAP) as supporting electrolyte in the potential range 1.2 to −1.2 V versus SCE at 100 mV s^{-1} scan rate (Table 3). The free ligands did not show any responses in the potential range scanned implying their redox innocent behavior. The complexes exhibited quasi-reversible one electron response (ΔE_p > 100 mV) corresponding to Fe(III)/Fe(II) couple with half wave potential ($E_{1/2}$), being negative. A relatively low $E_{1/2}$ values suggest easy redox susceptibility of the complexes. A representative voltammogram of the complex is displayed in Fig. 2. Our previous work on iron(III) complexes containing tetradentate $[N_2O_2]$ donor Schiff base ligand also showed quasi-reversible electrochemical behavior under identical conditions with similar ΔE_p values and negative half wave potential [33]. Pertinent here is to mention that quasi-reversible electrochemical behavior of iron(III) complexes containing Schiff bases are well documented [45–47]. Our recent publication also addressed quasi-reversible electrochemical nature of iron(III) complexes containing [ONO] donor tridentate Schiff base ligand [35].

3.9. Reactivity of the complexes

Reaction of the iron(III) complexes (**1** and **2**) with neutral nitrogen donor molecule imidazole, benzimidazole and pyridine in 1:2 molar ratio led to substitution of weakly held axial aquo groups affording new mixed ligand complexes (Scheme 3). Formation of the complexes (**3**–**8**) were confirmed by elemental analysis and spectroscopic data (Tables 4 and 5). The reactivity pattern thus provided access to an array of new complexes suggesting that this approach may be effectively employed involving other neutral or anionic donor molecules to afford variety of mixed ligand iron(III) complexes.

3.10. Quantum chemical calculations

Quantum-chemical calculations of two selected compounds viz. $[Fe(L^2)(H_2O)_2]^+$ and $[Fe(L^2)(Py)_2]^+$ were studied using DMOL3 software package [48]. Generalized Gradient approximation and DNP (Double Numerical Plus Polarization) basis set with BLYP functional were adopted in density functional theory (DFT) calculations. The sextet (s = 5/2) spin state was found to be energetically more stable than the doublet (s = 1/2) state, attesting the high-spin configuration of Fe^{3+} (d^5) as is also suggested by magnetic susceptibility measurements. The energy optimized structures of the complexes (Figs. 3 and 4) and the geometrical parameters (Table 6) suggest a distorted octahedral structure. The iron–oxygen (aquo) bond length (~2.4 Å) in $[Fe(L^2)(H_2O)_2]^+$ is quite longer than the iron–oxygen (Schiff base) bond length (~2.0 Å) validating the labile nature of metal-aquo linkages. The geometry of the complex $[Fe(L^2)(H_2O)_2]^+$ remains almost unaffected upon substitution of axial aquo groups.

The HOMO and LUMO energies of the complex $[Fe(L^2)(H_2O)_2]^+$ are found to be −3.692 and −2.566 eV (ΔE = 1.126 eV), respectively, while that for the complex $[Fe(L^2)(Py)_2]^+$ are −3.473 and −2.203 eV (ΔE = 1.270 eV), respectively. The HOMO–LUMO energy gap increases slightly on substitution of axial aquo groups in the complex $[Fe(L^2)(H_2O)_2]^+$ reflecting relatively higher stability of the substituted product.

4. Conclusion

Aquated iron(III)–Schiff base complexes of the type $[Fe(L^n)(H_2O)_2]NO_3$ have been synthesized from the reaction of $[N_2O_2]$ donor tetradentate Schiff bases (L^1 or L^2) with $Fe(NO_3)_3{\cdot}9H_2O$ and characterized by spectroscopic methods. The weakly bound water molecules at the axial coordination site of iron are readily replaced by neutral donor molecules leading to new mixed-ligand iron(III) complexes. Magnetic measurements and conductivity studies support a high spin (d^5) 1:1 electrolytic nature of the complexes. The complexes revealed quasi-reversible redox behavior with peak separation, ΔE_p > 100 mV. The TGA–DTA analysis data are consistent with the proposed structures and provided unambiguous evidence for coordinated water in the complexes. The synthetic strategy adopted is anticipated to open up new vistas for accessing vast array of new mixed-ligand complexes.

Acknowledgements

The authors thank to SAIF, NEHU, Shillong; SAIF, STIC, Kochi; CIF, IIT, Guwahati and SAIF, CDRI, Lucknow, India for providing analytical and spectral results. One of the author, Paritosh Mondal, thanks Department of Science and Technology, New Delhi for financial support (SR/FT/CS-86/2010).

Appendix A. Supplementary material

Supplementary data associated with this article can be found, in the online version, at doi:10.1016/j.ica.2011.12.056.

References

[1] V.K. Subramanian, M. Ganesan, S. Rajagopal, R. Ramaraj, J. Org. Chem. 67 (2002) 1506.
[2] H. Fuijii, T. Kurahashi, M. Sugimoto, K. Oda, T. Ogura, J. Inorg. Biochem. 96 (2003) 133.
[3] R.B. Bedfort, D.W. Bruce, R.M. Frost, J.W. Goodby, M. Hird, Chem. Commun. (2004) 2822.
[4] K.P. Bryliakov, E.P. Talsi, Angew. Chem., Int. Ed. 43 (2004) 5228.
[5] T. Katsuki, Chem. Soc. Rev. 33 (2004) 437.
[6] M.M. Bhadbhade, D. Srinivas, Polyhedron 17 (1998) 2699.
[7] S. Hayami, K. Inoue, Y. Maeda, Mol. Cryst. Liq. Cryst. 335 (1999) 573.
[8] W. Chiang, D. Vanengan, M.E. Thompson, Polyhedron 15 (1996) 2369.
[9] C.T. Brewer, G. Brewer, G.B. Jameson, P. Kamaras, L. May, M. Rapta, J. Chem. Soc., Dalton Trans. (1995) 37.
[10] H. Olmez, F. Arslan, H. Icbudak, J. Therm. Anal. Cal. 76 (2004) 793.
[11] D. Czakis-Sulikowska, J. Radwaska-Doczekalska, A. Czylkowska, A. Gouchowska, J. Therm. Anal. Cal. 78 (2004) 501.
[12] R. Carballo, A. Castineiras, S. Balboa, B. Covelo, J. Niclós, Polyhedron 21 (2002) 2811.
[13] J.B. Vincent, H.L. Tsai, A.G. Blackman, S. Wang, P.D.W. Boyd, K. Folting, J.C. Huffman, E.B. Lobkovsky, D.N. Hendrickson, G. Christou, J. Am. Chem. Soc. 115 (1993) 12353.
[14] C. Kaes, A. Katz, M.W. Hosseini, Chem. Rev. 100 (2000) 3553.
[15] G. Psomas, C. Dendrinou-Samara, P. Philippakopoulos, V. Tangoulis, C.P. Raptopoulou, E. Samaras, D.P. Kessissoglou, Inorg. Chim. Acta 272 (1998) 24.
[16] P. Losier, M.J. Zaworotko, Angew. Chem., Int. Ed. Engl. 35 (1996) 2779.
[17] R. Kruszynski, B. Kuznik, T.J. Bartczak, D. Czakis-Sulikowska, J. Coord. Chem. 58 (2005) 165.
[18] J. Li, Y. Zhang, J . Chen, L. Rui, Q. Wang, X. Wu, Polyhedron 19 (2000) 1117.
[19] J.H. Liao, S.H. Cheng, C.T. Su, Inorg. Chem. Commun. 5 (2002) 761.
[20] A.K. Saxena, J.K. Koacher, J.P. Tandon, Inorg. Nucl. Chem. Lett. 17 (1981) 229.
[21] P.G. Cozzi, Chem. Soc. Rev. 33 (2004) 410.
[22] S.K. Edulji, S.T. Nguyen, Organometallics 22 (2003) 3374.
[23] J.A. Miller, W. Jin, S.T. Nguyen, Angew. Chem., Int. Ed. 41 (2002) 2953.
[24] C. Celic, M. Tumer, S. Serin, Synth. React. Inorg. Met.-Org. Chem. 32 (2002) 1839.
[25] M.T. Kaczmarck, I. Pospieszna-Markiewick, W. Radecka-Paryzek, J. Incl. Phenom. Macro. Chem. 49 (2004) 115.
[26] S. Ilhan, H. Temel, A. Kilic, E. Tas, J. Cord. Chem. 61 (2008) 1443.
[27] S. Chandra, R. Kumar, Synth. React. Inorg. Met.-Org. Chem. 35 (2005) 161.
[28] S. Ilhan, H. Temel, I. Yilmaz, A. Kilic, Trans. Met. Chem. 32 (2007) 344.
[29] S.K. Gupta, P.B. Hitchcock, Y.S. Kushwah, J. Coord. Chem. 55 (2002) 1401.
[30] C.M. Che, J.S. Huang, Coord. Chem. Rev. 242 (2003) 97.
[31] F. Marchetti, C. Pettinary, R. Pettinary, A. Cingolari, D. Leonesi, A. Lorenzotti, Polyhrdron 18 (1999) 3041.
[32] M. Bagherzadeh, M. Amini, Inorg. Chem. Commun. 12 (2009) 21.
[33] C.R. Bhattacharjee, P. Goswami, P. Mondal, J. Coord. Chem. 63 (2010) 2002.
[34] C.R. Bhattacharjee, P. Goswami, M. Sengupta, J. Coord. Chem. 63 (2010) 3969.
[35] C.R. Bhattacharjee, P. Goswami, H.A.R. Pramanik, P.C. Paul, P. Mondal, Spec. Chim. Acta. Part A: Mol. Biomol. Spectrosc. 78 (2011) 1408.
[36] D.D. Perrin, W.L.F. Armarego, D.R. Perrin, Purification of Laboratory Chemicals, second ed., Pergamon Press, 1981.
[37] A. Gordon, R. Ford, S. Khimika, A Handbook of Practical Data, Techniques and References, John Wiley and Sons, Moscow, 1976.
[38] B. Chiswell, J.P. Crawford, E.J. O'reilly, Inorg. Chim. Acta 49 (1980) 223.
[39] N. Nawar, N.M. Hosny, Trans. Met. Chem. 25 (2000) 1.
[40] N. Raman, S. Ravichandran, C. Thangaraja, J. Chem. Sci. 116 (2004) 215.
[41] M.M. Abd-Elzahar, J. Chin. Chem. Soc. 48 (2001) 153.
[42] S.N. Rao, K.N. Munshi, N.N. Rao, M.M. Bhadbhade, E. Suresh, Polyhedron 18 (1999) 2491.
[43] A.B.P. Lever, Inorganic Electronic Spectroscopy, second ed., Elsevier, Amsterdam, 1984.
[44] W.J. Geary, Coord. Chem. Rev. 7 (1971) 81.
[45] R. Kannappan, S. Tanase, I. Mutikainen, U. Turpeinen, J. Reedijk, Polyhedron 25 (2006) 1646.
[46] A.D. Kulkarni, S.A. Patil, P.S. Badami, Int. J. Electrochem. Sci. 4 (2009) 717.
[47] H.H. Monfared, S. Sadighian, M.A. Kamyabi, P. Meyer, J. Mol. Catal. A: Chem. 304 (2009) 139.
[48] B. Delley, J. Chem. Phys. 92 (1990) 508.